Electronic Supplementary Material (ESI) for Physical Chemistry Chemical Physics.

Supplementary Information

Site Preference and Local Structural Stability of Bi(III) Substitution in Hydroxyapatite using First-Principles Simulations

Gerardo Martin Quindoza III[1], Yasuhiro Nakagawa[1], Hayato Laurence Mizuno[1,2], Yasutaka Anraku[1], Richard Espiritu[3], and Toshiyuki Ikoma[1]*

[1]Department of Materials Science and Engineering, School of Materials and Chemical Technology, Tokyo Institute of Technology, 2-12-1 Ookayama, Meguro-ku, Tokyo, Japan 152-8550

[2]Department of Biochemistry and Cellular Biology, National Center of Neurology and Psychiatry, 4-1-1 Ogawahigashicho, Kodaira-shi, Tokyo, Japan 187-0031

[3]Department of Mining, Metallurgical, and Materials Engineering, College of Engineering, University of the Philippines Diliman, Quezon City 1101, Philippines

*Corresponding Author: Toshiyuki Ikoma

E-mail address: tikoma@ceram.titech.ac.jp

Phone number: +81-3-5734-2519

Fax number: +81-3-5734-3369

S.1 Convergence test details

Before performing the geometry optimization calculations, a convergence test was conducted to ensure the accuracy of calculation using less calculation time. Convergence test was done by optimizing the cut-off value and the k-point sampling of the Brillouin zone. For faster optimizations, fluorapatite ($Ca_{10}(PO_4)_6F_2$; FAp) was used as model structure. The structure of FAp is very similar to hexagonal hydroxyapatite (HAp). The only difference between the two structures would be the anion in the screw-axis, wherein FAp have F^- ions while HAp have OH^- ions. Since the F^- ion in FAp can be found in the z = ¼ and ¾ mirror planes, first-principles calculations of the FAp structure are simpler and faster. The initial coordinates of FAp followed the results of Rulis *et al.* [1].

Initially, the conditions for GGA-PW91 functional were tested using various cut-off values ranging from 300 to 750 eV were tested using a constant k-point grid of 2×2×2. The final energy values of these runs are presented in Fig. S1. Fig. S1 shows that the final energy reached a stable value once the cut-off value reached 600 eV; therefore, it is set as the cut-off value for the geometry optimization of HAp.

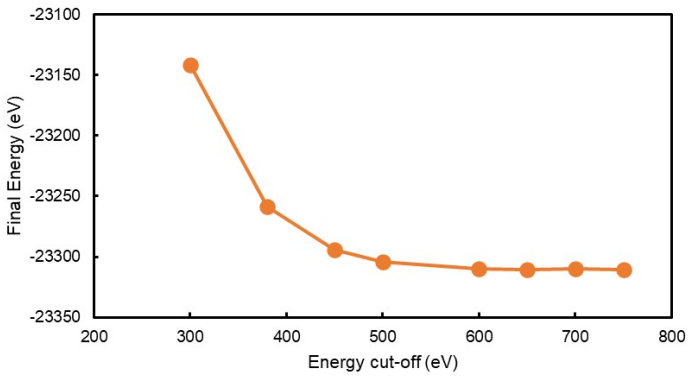

Fig. S1. Plot of final energy values of FAp model at varying energy cut-off and constant k-point grid of 2×2×2.

Using 600 eV, the value of k-point is optimized using the following test values: 1×1×2, 2×2×2, 2×2×4, 3×3×3, and 4×4×4. The plot of calculated final energies is shown in Fig. S2. It is evident that the final energies did not vary a lot. The 3×3×3 setting was chosen to ensure high

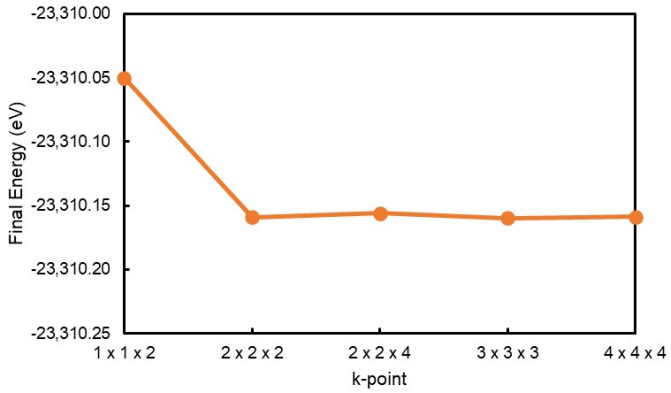

accuracy in calculations.

Fig. S2. Plot of final energy values of FAp model at varying k-point grids and constant energy cut-off of 600 eV.

Convergence test for the energy cut-off for the LDA/CA-PZ functional were also conducted. The results were presented in Fig. S3, and it is evident that a stable value can be obtained at 600 eV. The energy cut-off was chosen to be 600 eV and the k-point was

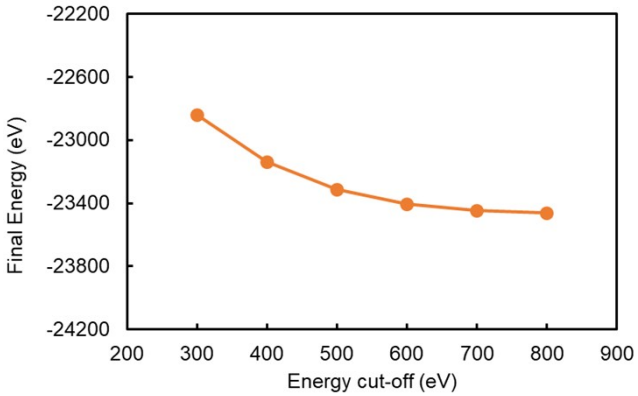

maintained at 3x3x3 for the phonon calculations.

Fig. S3. Plot of final energy values of FAp model at varying energy cut-off and constant k-point grid of 2×2×2 using LDA/CA-PZ functional.

S.2 Supplementary Bi(III) substituted HAp models

It was discussed in section 2-2 of the main text that the number of model structures were decreased due to equivalency of some models. For the assumption that the position of O and OH groups above or below the mirror plane results in equivalent structures, three test models were selected. The Bi(1)HAp O model was used as reference with the arrangement of O and OH hydroxyl ions shown in Fig. S3a. The two other models have (1) O below z = ¼ and OH above z = ¾ (labeled as Bi(1)HAp HO-O) and (2) O above z = ¼ and OH below z = ¾ (labeled as Bi(1)HAp OH-O), as shown in Fig. S3b and S3c, respectively.

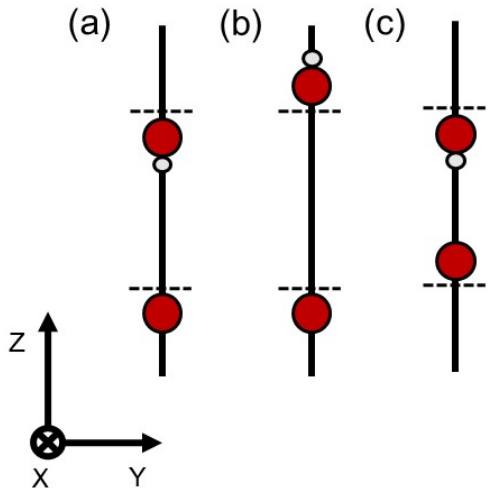

Fig. S4 Illustration of hydroxyl channel of (a) Bi(1)HAp O (reference), (b) Bi(1)HAp with O below z = ¼ and OH above z = ¾, (c) Bi(1)HAp with O above z = ¼ and OH below z = ¾.

Table S1 summarized the final energy values of the three models. It is very evident that the final energy values are almost equal, and the position of O and OH groups can be practically ignored.

Table S1. Final energy values of Bi(1)HAp O model, Bi(1)HAp HO-O (O below z = ¼ and OH above z = ¾), and Bi(1)HAp OH-O (O above z = ¼ and OH below z = ¾).

Model Name	Final Energy per atom (eV/atom)
Bi(1)HAp O	-558.6125
Bi(1)HAp HO-O	-558.6148
Bi(1)HAp OH-O	-558.6123

Table S2. Final energy values of Bi(1)HAp O, Bi(1)HAp OH, Bi(2)HAp O, and Bi(2)HAp OH models using LDA/CA-PZ functional.

Model Name	Final Energy per atom (eV/atom)
Bi(1)HAp O	-557.9774
Bi(1)HAp OH	-557.9803
Bi(2)HAp O	-557.9994
Bi(2)HAp OH	-557.9995

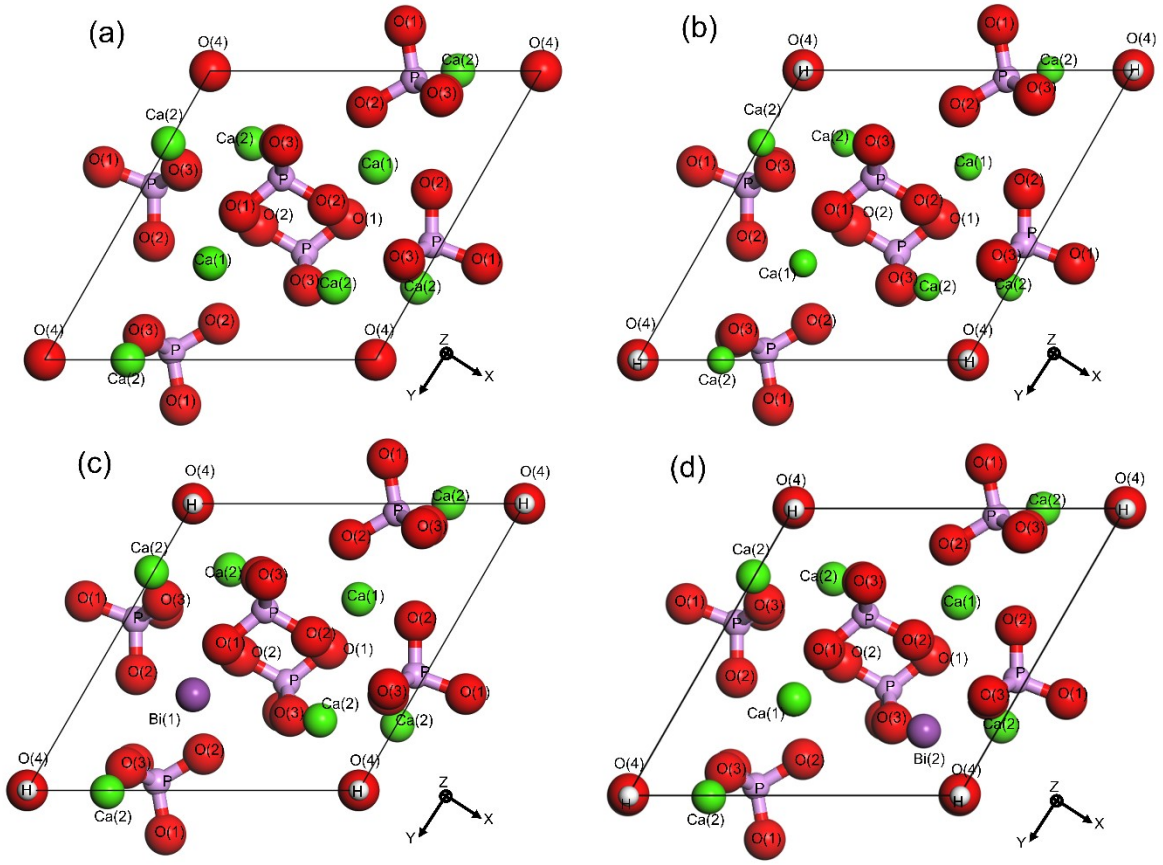

Fig. S5. Optimized structures of the following models (bottom view/XY plane view): (a) HAp H (OH-HO arrangement), (b) HAp O (HO-OH arrangement), (c) Bi(1)HAp OH (Bi^{3+} near OH), and (d) Bi(2)HAp OH (Bi^{3+} near OH).

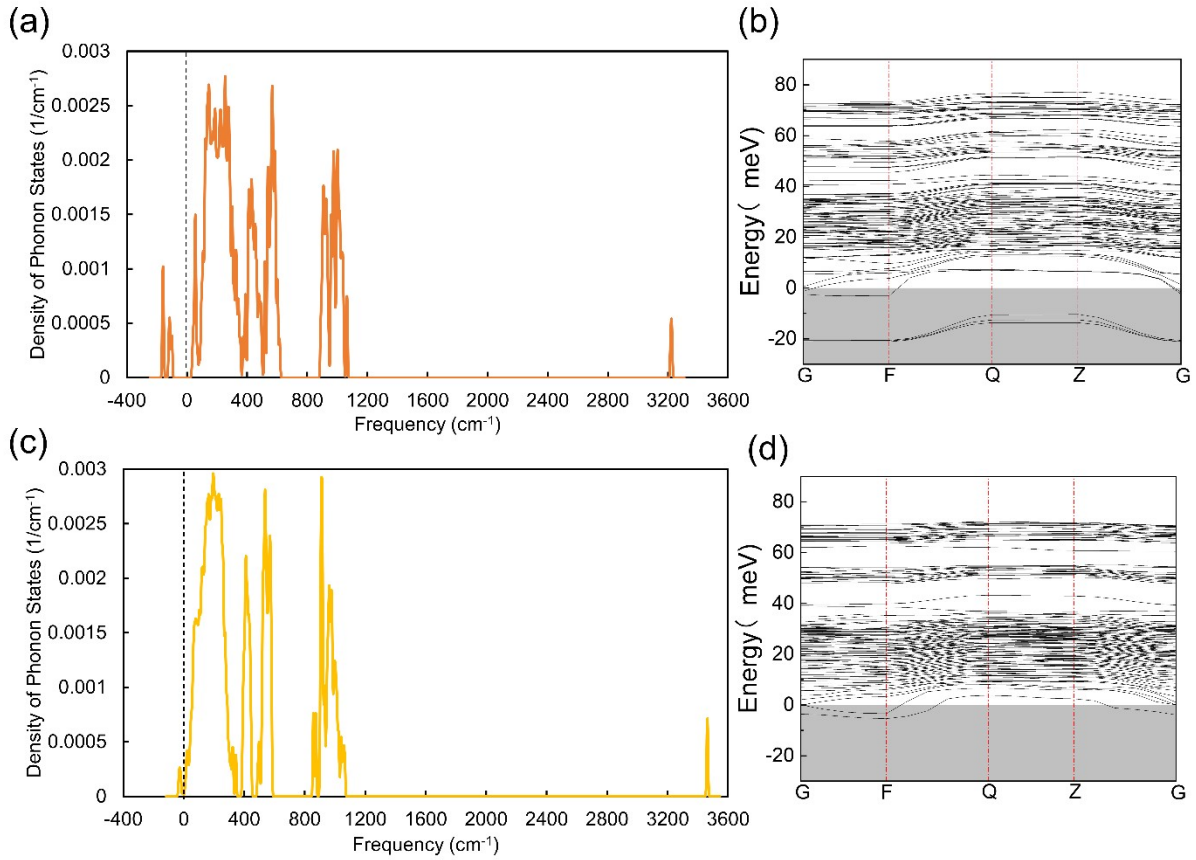
(a)
Density of Phonon States (1/cm-1)
0.003
0.0025
0.002
0.0015
0.001
0.0005
0
-400
0
400
800
1200
1600
2000
2400
2800
3200
3600
Frequency (cm-1)
(b)
Energy(meV)
80
60
40
20
0
-20
G
F
Q
Z
G
(c)
Density of Phonon States (1/cm-1)
0.003
0.0025
0.002
0.0015
0.001
0.0005
0
-400
0
400
800
1200
1600
2000
2400
2800
3200
3600
Frequency (cm-1)
(d)
Energy(meV)
80
60
40
20
0
-20
G
F
Q
Z
G

Fig. S6. Phonon density of states and phonon dispersions of the (a, b) Bi(1)HAp O and (c, d) Bi(2)HAp O models using the GGA-PW91 functional.

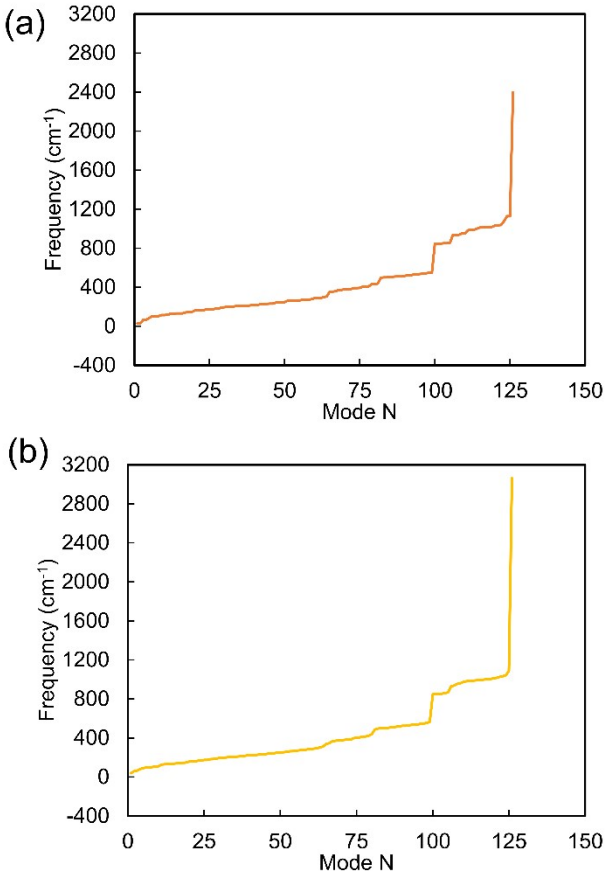

Fig. S7. Summary of calculated vibrational frequencies of (a) Bi(1)HAp O and (b) Bi(2)HAp O models using the LDA/CA-PZ functional.

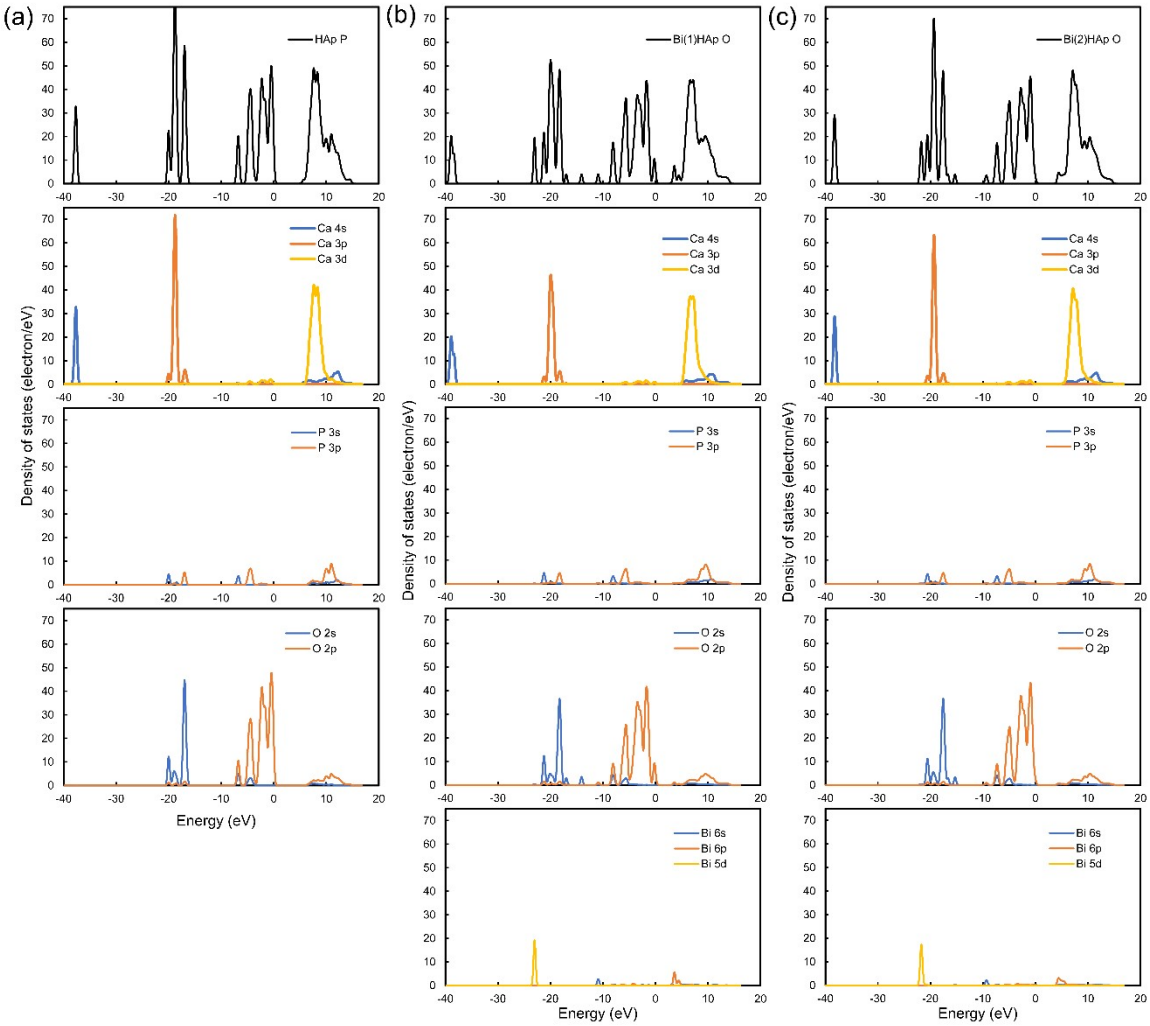

Fig. S8. Total density of states (DOS) and partial density of states (PDOS) plots of (a) HAp P, (b) Bi(1)HAp O, and (c) Bi(2)HAp O models.

References

1 P. Rulis, L. Ouyang and W. Y. Ching, Electronic structure and bonding in calcium apatite crystals: Hydroxyapatite, fluorapatite, chlorapatite, and bromapatite, *Phys. Rev. B - Condens. Matter Mater. Phys.*, 2004, **70**, 1–8.